

Removal of Manganese Ion Using Integral Membrane Incorporated with Rice Husk Ash

Norin Zamiah Kassim Shaari^{1*}, Nabilah Huda Alias¹, Nurul Atirah Fitriah Mohd Zainuddin¹, Nur Syazwanie Izzati Chik¹

¹*School of Chemical Engineering, College of Engineering, Universiti Teknologi MARA 40450 Shah Alam, Selangor, Malaysia*

*Corresponding author's E-mail: norinzamiah@uitm.edu.my

Received: 12 November 2022

Accepted: 06 February 2023

Online First: 17 March 2023

ABSTRACT

Wastewater treatment is a method of ensuring that the water supply is clean and free from contaminants. Manganese is a pollutant that needs to be removed from the water as it is harmful and usually triggers concern about water quality and water distribution system issues. Besides the adsorption method, membrane technology is efficient due to its mild and environmentally friendly process. This research focused on the production of integral membranes from a blend of polyvinyl alcohol/chitosan/polysulfone/polyethylene glycol cross-linked with silica extracted from rice husk ash (RHA) by using the phase inversion method. The silica was incorporated into the membrane formulation through a sol-gel reaction. The goal of this research was to determine the potential utilization of silica from RHA in the membrane's formulation to remove manganese ions from various concentrations of manganese solutions. The loadings of RHA were varied at 2, 3 and 5 % wt./wt. polymer. The formulated membranes were then characterized in terms of thermal stability by Thermogravimetric analysis, functional group by Fourier Transform Infrared Spectroscopy, and surface morphology by Scanning Electron Microscopy. The performances of the membranes were tested through filtration of manganese ions solutions and antifouling analysis. The results showed that all membranes including membranes from the polymer blend were able to remove more than 94 % manganese ions. However, the membrane incorporated with 2 % RHA portrayed the best performance in terms of obtaining the highest flux for both water and manganese as feed solution respectively, which also resulted



in the highest relative flux recovery ratio at 62.50 % from the antifouling analysis. These findings have proven the successful incorporation of RHA in the form of silica powder, which shows the potential utilization of RHA in membrane fabrication.

Keywords: Antifouling; integral membrane; manganese ion; rice husk ash

INTRODUCTION

Water is a valuable and necessary component for all living beings that must be preserved in terms of quality. However, the rapid industrial expansion has caused the water to be contaminated by waste discharged from industrial, domestic, and commercial sources. This includes the discharge of heavy metals into the water supply, either directly or indirectly [1]. The chemical nature of metal ions determines their potential toxicity when they enter the water. It has the potential to harm aquatic species as well as human health [2]. Manganese as one of the heavy metals has been found in drinking water supplies, where sometimes its concentration exceeds the secondary standard maximum contamination levels (MCLs) at 0.1 mg/L [2]. To cater to the pollution resulting from a discharge of manganese, it must be removed from water using an appropriate treatment method and technology. There are various methods for the removal process which include membrane filtration, oxidation, adsorption, ion exchange, precipitation, and coagulation. Adsorption is a widely used technique because it is cheaper, environmentally friendly, safe, and easy to operate [3]. Furthermore, adsorption using activated carbon is highly efficient for the removal of impurities or pollutants from wastewater. However, the high cost of activated carbon is a drawback when a larger scale of applications is required. This situation has resulted in membrane separation becoming the preferable choice due to its mild, environmentally friendly process and does not generate sludge. Furthermore, membrane technology requires smaller equipment size, cheaper capital cost, and energy demand, and it has the potential to bridge the economic and sustainability gaps, as it uses no chemicals and is accessible to a wide range of people [4]. Apart from the microfiltration (MF) membrane, there are a few major types of membrane processes for treating heavy metal-contaminated water which are complexation-enhanced UF (CEUF), micellar-enhanced UF (MEUF),

and adsorptive UF mixed matrix membranes (UFMMMs) [5].

The incorporation of biomass as a filler in the membrane's formulation is one way to enhance the adsorption efficiency of the membrane subjected to the type of filler. Rice husk ash as biomass from rice production has been widely used as a filler for membranes due to its abundance and contains 95 wt.% silica [6]. Rice husk is granular in shape, insoluble in water, and chemically and mechanically stable. The rice husk ash (RHA) is the product when the rice husk goes through the combustion process in the incinerator. In the controlled combustion process that operates with a temperature of 500-700 °C for 1 hour, the amorphous silica is generated as a major constituent of ash which illustrates the existence of silica composition. The surface area of amorphous silica is large due to the structure of microporous ash particles [7]. It has a non-uniform shape with a diameter ranging from less than 1 micron to microns but most of them are being in 45 microns in size [8]. In addition, the amount of silica inside the rice husk ash (RHA) varies since it depends on several variables such as rice moisture content, type of furnace, combustion condition, geographical conditions, and regional climate [9]. Rice husk ash (RHA) is labelled as one of the precursor materials that can be used as a filler for the membrane in the adsorption process of contaminants from wastewater since rice husk ash (RHA) is the waste from the rice industry and its utilization in membrane formulation could promote the reduction in the environmental impact caused by rice husk ash (RHA) accumulation [10]. As reported by Alias et al., 2020 [10], besides functioning as a filler, rice husk ash (RHA) acts as a cross-linker for hybrid membrane production due to its reactive amorphous silica structure. In addition, the RHA has been known to contain several functional groups that contribute advantages as biosorbents such as carboxyl, hydroxyl, phosphate, sulfate, ether, and amino acids [11].

With regards to manganese ion removal, it has been reported that RHA has been utilised as a bio-sorbent in the biosorption studies that were carried out using a shaker machine with a revolving speed of 130 rpm at 25 °C and 150 mL flasks holding 50 mL of manganese solutions at 5 to 40 ppm [2]. An acid-cleaned 0.45 m Millipore filter was used to filter the mixture. Results showed that 96 % removal of manganese ions was achieved at pH 6 at 0.6 g/100 mL of RHA loading. Based on this promising result of the adsorption process, it is therefore this study aimed to investigate the manganese removal

efficiency through a formulated membrane that was incorporated with extracted silica powder from RHA. The membrane was formulated from a polymer blend of polyvinyl alcohol/chitosan/polysulfone/polyethylene glycol. The thermal stability, functional group, surface morphology, and antifouling properties of the membranes were tested. This separation process represented the integrated complexation process because the adsorption of manganese ions and the subsequent removal from the feed solution occurred simultaneously on the membrane's surface.

METHODOLOGY

Materials

Polyvinyl alcohol, 87-89 percent hydrolyzed with MW 85000-124000, and polysulfone with MW 22000 were purchased from Sigma Aldrich (M) Sdn Bhd, Subang, Malaysia. Chitosan (CS) was purchased from Aman Semesta Enterprise, Shah Alam, Malaysia. 1-methyl-2-pyrrolidone (NMP) and polyethylene glycol 400 were purchased from Merck Sdn Bhd, Selangor, Malaysia. Hydrochloric acid (37 % purity), dimethyl sulfoxide, and humic acid were purchased from R&M Chemicals, Subang, Malaysia. Rice husk ash was purchased from BT Science Sdn Bhd, Selangor. Sodium hydroxide, acetic acid, and deionized water were obtained from Chemical Laboratory at the College of Engineering, Universiti Teknologi MARA (UiTM) Shah Alam, Malaysia.

Preparation of blend membrane solution

10 g of polyvinyl alcohol (PVA) powder was dissolved into 90 g of dimethyl sulphoxide followed by heating at 90 °C for 4 hours with continuous stirring at 400 rpm until a homogeneous solution was obtained. After that, it was cooled down to room temperature. For the preparation of 2 wt.% chitosan solution, 0.02 g of chitosan was dissolved in 99.98 g of aqueous acetic acid followed by heating at 90 °C for 4 hours with continuous stirring at 400 rpm. It was then left at room temperature [12].

Preparation of hybrid membranes

Both prepared solutions of PVA and chitosan respectively were mixed at a weight ratio of 1:1 and heated at 60 °C for 7 hours while stirring constantly at 400 rpm. Extracted silica powder from RHA powder was added at a concentration of 2 wt.% [13]. The method of silica powder extraction from the RHA was disclosed in the previous work [14]. The composition of the silica powder is depicted in Table 1 [14]. For the sol-gel technique, 1 mL of HCl was added as a catalyst. The solution was then allowed to cool to room temperature. The steps above were repeated by using 3 wt.% and 5 wt.% of RHA powder, and another membrane was prepared without the addition of RHA. The composition of each formulation is shown in Table 2.

Table 1: Composition of silica powder from RHA

Compound	Percentage (%)
Si	77.02
Na	0.49
Cl	0.53
Other impurities	21.97

Table 2: Composition of various membrane solutions

Membrane code	PVA solution (g)	CS solution (g)	RHA powder (wt./wt.% polymer)
0 RHA	50	50	0
2 RHA	50	50	2
3 RHA	50	50	3
5 RHA	50	50	5

Preparation of polysulfone (PSF) solution

13 g of polysulfone beads were dissolved in 82 g of 1-methyl-2-pyrrolidone (NMP) and then followed with the addition of 5 g polyethylene glycol. For approximately 6 hours, the solution was heated and stirred continuously at 60°C at 400 rpm. The mixture was then allowed to cool to room temperature [12].

Preparation of the integral membrane

1 g from each of the hybrid membrane solutions was added to a 50 g PSF solution respectively. The mixture was stirred at 700 rpm for 3 hours while being heated to 80 °C. After cooling down, the solution was poured onto a glass plate and spread to a thickness of 100 µm with a Baker Film Applicator. The plate was then soaked for 24 hours in a large amount of water. After that, the membrane was dried for 24 hours at room temperature [12, 15].

Characterizations of membrane

Thermogravimetry analysis (TGA) was used to evaluate the thermal stability of the fabricated membranes, which was measured through degradation temperature and the weight residue. Small pieces of the membrane were prepared with weight ranges from 5 to 10 mg. The membranes were heated at a rate of 10 °C/min from 0 °C to 900 °C under a nitrogen atmosphere [12]. The TGA model used was from the Mettler Toledo model Stare SW.

The functional groups of the integral membrane were identified through FTIR analysis. From the generated infrared absorption spectrum, the analysis identifies the presence of chemical bonds in the membrane. FTIR Spectrometer with Model Spectrum 400 from the Perkin Elmer Spectrum One was used. The wavelength was measured between 400 cm⁻¹ and 4000 cm⁻¹ [16].

The surface morphology of the membrane was identified by using a Scanning Electron Microscopy (SEM) instrument, Hitachi SU3500 (351716-01). Before the analysis, the membranes were coated with copper to reduce the electric charge. The accelerating voltage was adjusted to 15 kV with a magnification of ×1.5k. The surface images of 0 RHA and 2 RHA membranes were captured and investigated.

Performance of membranes

The fabricated dead-end filtration rig was used for the performance test on manganese removal and antifouling analysis. The manganese solutions were prepared at 5, 10, and 15 ppm by using deionized water and dilution method from 100 ppm manganese solution. The pressure was set at 6 bars using nitrogen gas. For each piece of membrane, 2 hours of filtration time was performed with 30 minutes intervals of sampling. Flux was measured every 30 minutes from the withdrawn sample solution according to Equation 1.

$$Flux = \frac{\Delta V}{A\Delta t} \quad (1)$$

Where ΔV is the volume of the collected permeate solution, A is the cross-sectional area of the membrane, and Δt is the interval time.

The concentration of manganese in feed (C_f) and permeate stream (C_p) respectively, was measured using Atomic Absorption Spectroscopy (AAS) from Mettler Toledo [17]. The percentage rejection of manganese ions from the feed solution was calculated according to Equation 2.

$$Rejection \% = \frac{C_f - C_p}{C_f} \times 100 \quad (2)$$

For the antifouling experiment, 10 bars of pressure from nitrogen gas were set [18]. The process was carried out in three stages. Humic acid solution as the foulant model was prepared by dissolving 2 g of humic acid in 1 L of 200 ppm sodium hydroxide. In the first stage, deionized water was used as the feed solution, and the filtration was performed in 30 minutes. The permeate stream was continuously withdrawn and the final flux was measured and labeled as J_o . The process was continued by replacing deionized water with humic acid solution and the process was performed for 2 hours. A sampling of permeate was done for every 20 minutes for 2 hours. At the end of the 2-hour filtration process, the flux was measured and labeled as J_p . The membrane was taken out from the casing of the stirred cell and it was backwashed by soaking the membrane in 50 mL water where the magnetic bar was placed on the membrane. Stirring was performed at 150 rpm, and the process last for 30 minutes. The last

stage was performed by repeating the first stage and the flux was labeled as J_1 . The antifouling properties were measured in terms of relative flux decay (RFD) and relative flux recovery (RFR) according to Equation 3 and Equation 4 respectively [19].

$$RFD = \frac{(J_0 - J_p)}{J_0} \times 100 \quad (3)$$

$$RFR = \left(\frac{J_1}{J_0}\right) \times 100 \quad (4)$$

RESULT AND DISCUSSION

Thermal stability

The results from the TGA analysis are plotted in Figure 1. Generally, there were three stages of the weight loss profile portrayed by the 0 RHA membrane but only two stages were significantly portrayed by membranes incorporated with silica from RHA. Based on the figure, for 0 RHA membrane, the degradation started at 100 °C, which showed less thermal stability of the membrane as compared to the membrane with RHA that started to degrade at a higher temperature. The elimination of the hydroxyl group from PVA and chitosan was portrayed through the second stage of weight loss around 400 °C to 600 °C [20]. At this stage, the 0 RHA membrane suffered from the highest weight loss as compared to other membranes. The degradation of the polymer backbones in the membrane was shown through the final weight loss profile after 600 °C where membranes with RHA have slightly decreased in weight as compared to the 0 RHA membrane where a drastic fall in the weight residue was observed for 0 RHA [20]. Furthermore, as the RHA content increases, the membrane weight residue steadily increases, where 5 RHA displayed the highest weight residue. This situation was attributed to the presence of inorganic silica from RHA that has considerably stabilized the membranes' heat deterioration as a result of the crosslinking reaction between the hydrogen bond from polymers with the silica from RHA [20]. Higher loading of RHA provides strong interaction between the polymer matrix of the polymer blend with the silica through a covalent bond, which has high activation energy. As a result, the membrane

becomes more thermally resistant and harder [21].

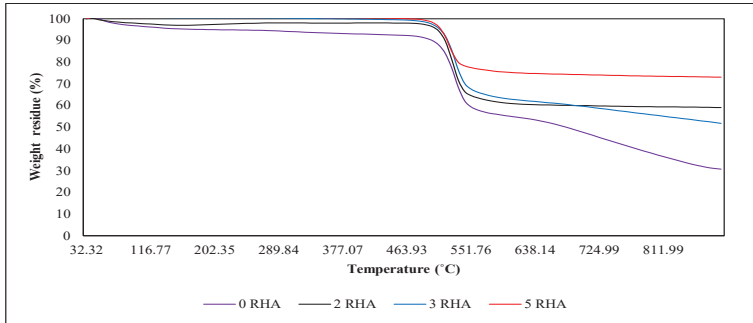


Figure 1: Percentage weight residue of membranes at different temperatures

Functional group of membranes

The results from the FTIR analysis were shown in Figure 2(a)-2(d). As can be observed from each figure, a large number of peaks are found, where there were similar peaks in the spectra that depict the membrane's fingerprint, which consists primarily of polysulfone, polyvinyl alcohol, chitosan, and rice husk ash that mostly falls in the region of $400\text{-}1500\text{ cm}^{-1}$ [22]. Si-O-Si and Si-O absorption bands from rice husk ash were discovered between 1016 cm^{-1} and 835 cm^{-1} [10, 23]. The peak at 2976 cm^{-1} corresponded to C-H stretching that overlapped with amine bands [12]. A broad absorption band was discovered between $3000\text{ to }3750\text{ cm}^{-1}$ as shown in Figure 2(d) representing the hydroxyl groups from all membranes where the intensity decreases with the increase in loading of silica powder in the membrane's formulation [22].

A large and steep peak was discovered in the double bond region ($1500\text{-}2000\text{ cm}^{-1}$), which indicated the presence of a carbonyl double bond. Several peaks at 1600 cm^{-1} indicate C=C bonding in the material [22]. The vibration modes of C=O and C-O bonds from unhydrolyzed vinyl acetate from PVA have contributed to the peaks evolution between 1200 cm^{-1} and 1700 cm^{-1} [12]. For the membrane incorporated with silica powder, the spectrum adsorption of Si-C and Si-O bonds have overlapped the initial C-O bond, forming Si-O-C at 1016 cm^{-1} as shown in Figure 2(a), which proofing the crosslinking reaction in the membrane [24]. The peak intensity also increases with the increase in the loading of RHA silica powder.

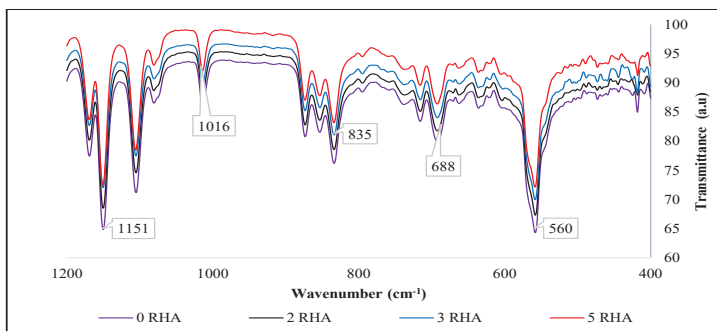


Figure 2(a): FTIR Analysis between 400-1200 wavenumber (cm⁻¹)

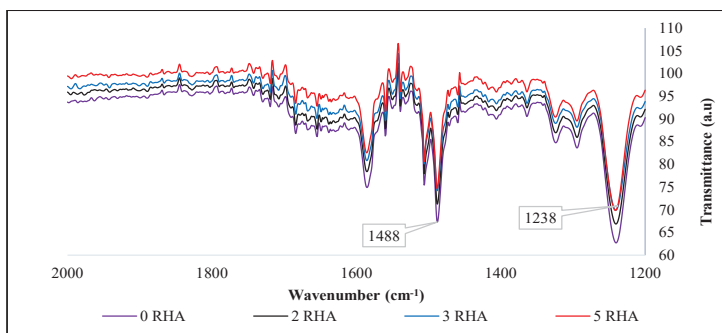


Figure 2(b): FTIR Analysis between 1200-2000 wavenumber (cm⁻¹)

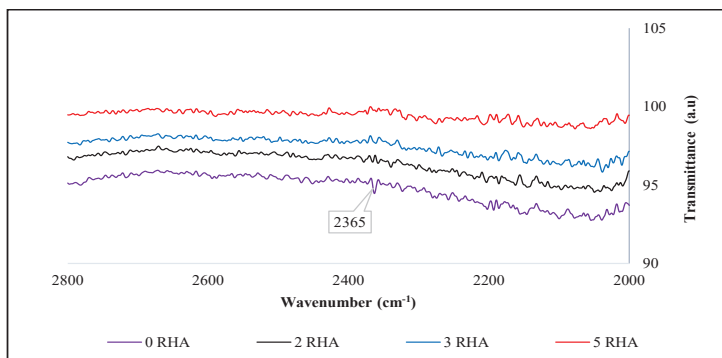


Figure 2(c): FTIR Analysis between 2000-2800 wavenumber (cm⁻¹)

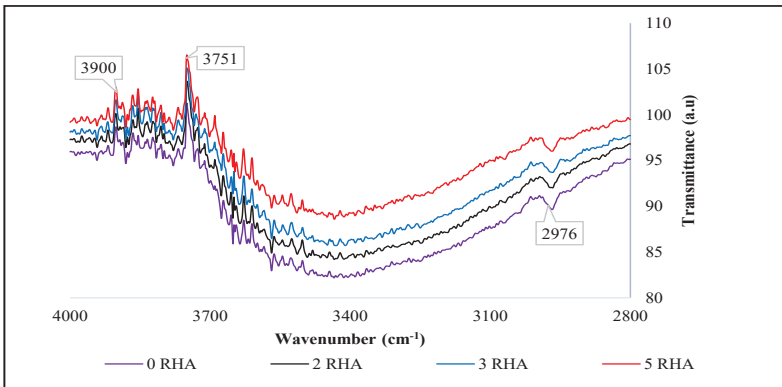


Figure 2(d): FTIR Analysis between 2800-4000 wavenumber (cm⁻¹)

Surface morphology from SEM analysis

As shown in Figures 3 (a) and (b), the presence of RHA tightened the matrix structure of the membrane, where a denser surface was observed for 2 RHA as compared to 0 RHA. This dense structure was attributed to the crosslinking reaction between silica from RHA and the hydroxyl group in the polymer matrix [13].

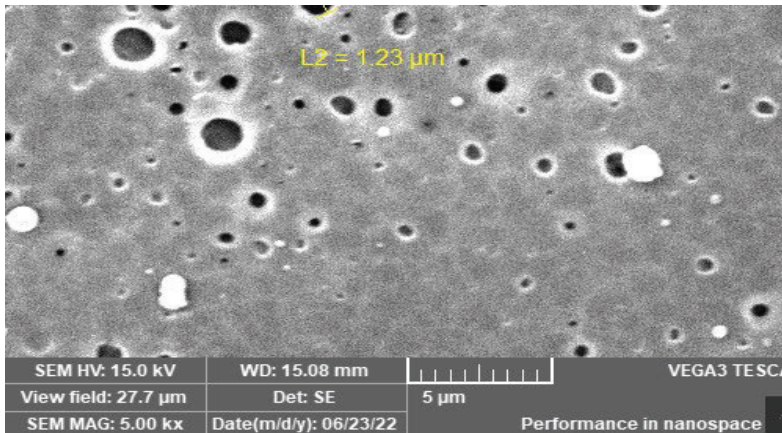


Figure 3 (a): The surface image of membrane 0 RHA

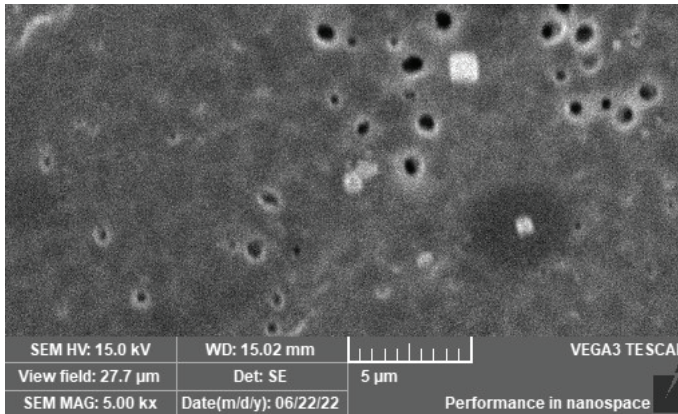


Figure 3(b): The surface image of membrane 2 RHA

Manganese removal and its flux

Figure 4(a), 4(b), and 4(c) show the permeation fluxes from the manganese removal process at various manganese feed concentrations. Based on these three figures, the fluxes consistently decreased after 30 minutes of filtration for all membranes. Despite the compact structure due to crosslinking with silica from RHA as shown from SEM analysis, membrane 2 RHA had the highest flux for all concentrations of manganese solution that had surpassed with that obtained from membrane 0 RHA. As there were no obvious enlarged pores on the membrane's surface after the filtration process, it showed the membranes did not swell [25]. This situation demonstrated that the denser structure of the membrane due to the crosslinking reaction has strengthened the membrane structure and increased membrane stability [26]. Furthermore, the exhaustion of the hydroxyl group due to cross-linking process with silica did not affect the 2 RHA membrane due to the hydrophilic nature of silica that compensates for this situation, resulting in a higher water permeability as compared to that of the 0 RHA membrane [10, 27].

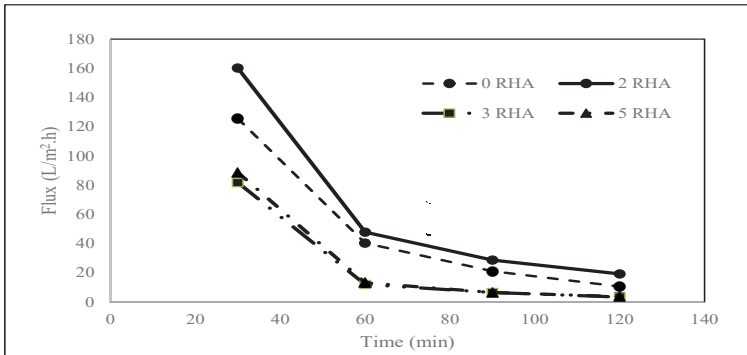


Figure 4(a): Flux from filtration of 5 ppm manganese solution

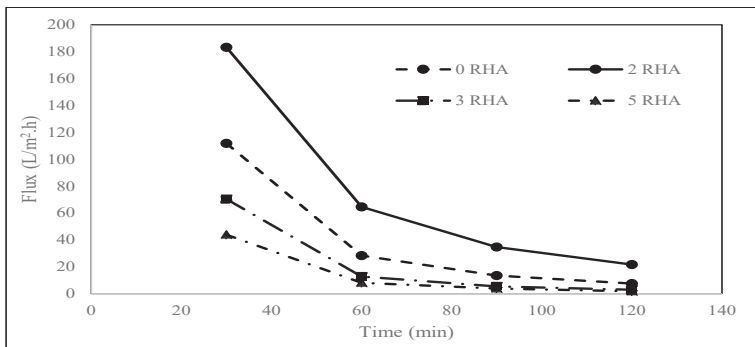


Figure 4(b): Flux from filtration of 10 ppm manganese solution

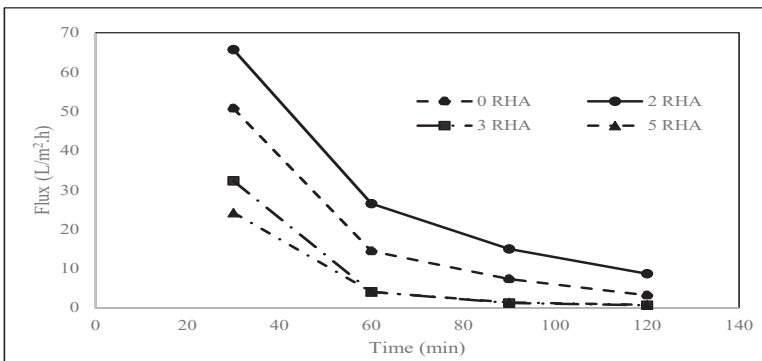


Figure 4(c): Flux from filtration of 15 ppm manganese solution

In terms of the membranes' performance to adsorb manganese ions, the percentage removal of manganese ions from various concentrations of the feed solution was shown in Table 2. Based on the table, the comparable removal efficiency was portrayed by all membranes where more than 90 % of manganese could be removed even in the early 30 minutes of filtration time. However, a significant result could be observed for 15 ppm manganese feed solution where membranes 3 RHA and 5 RHA have removed almost 100 % manganese ions respectively after 2 hours of filtration time. This result was caused by a large surface area for ions adsorption due to pore tightening as a result of a rapid cross-linking reaction as can be observed from SEM analysis. The build-up layer of the adsorbed ion creates concentration polarization that explains the flux reduction for 3 RHA and 5 RHA as depicted by Figure 4(a)-4(c). The percentage removal of manganese ions was comparable to that obtained from the research by using the biosorption process [2].

Table 2: Percentage removal of manganese ions at various filtration times and using various formulations of membrane

Feed concentration of Manganese (ppm)	Membrane code	Filtration time			
		30 min	60 min	90 min	120 min
		Manganese removal (%)			
5	0 RHA	94.94	95.15	95.22	95.06
	2 RHA	95.23	95.30	95.71	95.30
	3 RHA	95.31	94.95	95.49	95.13
	5 RHA	95.25	95.42	95.72	95.32
10	0 RHA	95.50	95.58	95.53	95.52
	2 RHA	94.77	94.84	94.75	94.77
	3 RHA	94.74	94.70	94.72	94.75
	5 RHA	95.08	94.84	94.83	94.80
15	0 RHA	94.08	94.11	94.04	94.03
	2 RHA	93.99	93.98	94.01	94.02
	3 RHA	94.06	93.91	94.00	98.80
	5 RHA	93.99	93.93	93.91	98.63

Antifouling performance

The antifouling properties of the membranes were assessed using a humic acid (HA) solution as the foulant model to simulate the natural organic matter in the actual environment. The values of J_o , J_p , and J_f for each membrane were depicted in Table 3. Based on the table, all membranes had identical flux dropping rates for filtration of HA solution. Membrane 2 RHA had the highest flux throughout three hours of the filtration period regardless of the type of solution. Although membrane 2 RHA had the highest relative flux decay, it was compensated by its higher relative flux recovery. High relative flux recovery showed increased hydrophilicity of the membrane's surface, which lessened the effect of the concentration polarization phenomenon.

Table 3: Antifouling properties of membranes from various formulations

Membrane code	J_o (L/m ² .h)	J_p (L/m ² .h)	J_f (L/m ² .h)	RFD (%)	RFR (%)
0 RHA	47	3.6	26	92.34	55.32
2 RHA	240	11.8	150	95.08	62.50
3 RHA	59	3.1	31	94.75	52.54
5 RHA	37	3.15	10	91.49	27.03

CONCLUSION

The presence of RHA in the matrix of the integral membrane had been found to improve the thermal stability of the membranes, increase the percentage removal of manganese ions which was significantly shown at high manganese ions concentrations, and enhanced the antifouling properties of the membrane. The best concentration of silica powder from RHA incorporated in the membrane was 2 RHA which has led to a higher permeation flux and portrayed good antifouling properties. Good integral stability of the membrane incorporated with silica powder was resulted from the cross-linking process. These findings show a potential utilization of RHA in membrane fabrication for the treatment of wastewater. Furthermore, the stiffer membrane was a preferable property to undergo rough conditions during actual operation.

ACKNOWLEDGMENT

The authors would like to thank the College of Engineering, UiTM Shah Alam for providing the laboratory facilities and equipment to carry out this research and perform the analysis respectively. Thank you also to En. Nazmi Mukhlas for helping in the analysis of manganese concentration using AAS. Thank you to Prof. Dr. Azni Zain Ahmed for proofreading this article.

REFERENCES

- [1] N.N. Rudi, M.S. Muhamad, L.T. Chuan, J. Alipal, S. Omar, N. Hamidon, N.H.A. Hamid, N.M Sunar, R. Ali, H. Harun, 2020. Evolution of adsorption process for manganese removal in water via agricultural waste adsorbents. *Heliyon*, vol. 6 (9), pp. 1-13.
- [2] Y. Zhang, J. Zhao, Z. Jiang, D. Shan, Y. Lu, 2014. Biosorption of Fe(II) and Mn(II) ions from aqueous solution by rice husk ash. *BioMed Research International*, vol. 2014, pp. 1-10.
- [3] R. Mu, B. Liu, X. Chen, N. Wang, J. Yang, 2020. Hydrogel adsorbent in industrial wastewater treatment and ecological environment protection. *Environmental Technology & Innovation*, vol. 20, pp. 101107.
- [4] A. Zirehpour, A. Rahimpour, 2016. Chapter 4: Membranes for wastewater treatment: Applications, in book *Nanostructured Polymer Membranes*, pp. 159-207.
- [5] N. Abdullah, N. Yusof, W.J. Lau, J. Jaafar, A.F. Ismail, 2019. Recent trends of heavy metal removal from water/wastewater by membrane technologies. *Journal of Industrial and Engineering Chemistry*, vol. 76, pp. 17-38.
- [6] M. Ahmaruzzaman and V. K. Gupta, 2011. Rice husk and its ash as low-cost adsorbents in water and wastewater treatment. *Industrial & Engineering Chemistry Research*, vol. 50 (24), pp. 13589-13613.

- [7] R. Siddique and P. Cachim, 2018. Waste and Supplementary Cementitious Materials in Concrete: Characterisation, Properties, and Applications: Chapter 13 - Rice husk ash, by B. Singh, *Woodhead Publishing, Cambridge, United Kingdom*.
- [8] B. I. Rasoul, 2018. The effect of rice husk ash on the mechanical and durability properties of concrete. Student thesis: *Doctoral thesis. School of Environment and Technology in University of Brighton, United Kingdom*.
- [9] T. Hongo, J. Sugiyama, Atsushi Yamazaki, Akihiro Yamasaki, 2013. Synthesis of aluminosilicate nanotube from rice husk ash and its characterization. *Nanopages*, vol. 8 (1), pp. 9-14.
- [10] S.S. Alias, Z. Harun, N. Manoh, M.R. Jamalludin, 2020. Effects of temperature on rice husk silica ash additive for fouling mitigation by polysulfone-rhs ash mixed-matrix composite membranes. *Polymer Bulletin*, vol. 77 (8), pp. 4043-4075.
- [11] N.S. Zainal, Z. Mohamad, M.S. Mustapa, N.A. Badarulzaman, A.Z. Zulkifli, 2019. The ability of crystalline and amorphous silica from rice husk ash to perform quality hardness for ceramic water filtration membrane. *International Journal of Integrated Engineering*, vol. 11 (5), pp. 229-235.
- [12] N.A. Sulaiman, N.Z.K. Shaari, and N.A. Rahman, 2016. Removal of CU (II) and FE (II) ions through thin film composite (TFC) with hybrid membrane. *Journal of Engineering Science and Technology*, vol. 11, pp. 36-49.
- [13] C. Mbareck, Q.T. Nguyen, O.T. Alaoui, D. Barillier, 2009. Elaboration, characterization and application of polysulfone and polyacrylic acid blends as ultrafiltration membranes for removal of some heavy metals from water. *Journal of Hazard Material*, vol. 171 (1-3), pp. 93-101.
- [14] N.S.I. Chik, N.Z. Kassim Shaari, N.A. Ramlee, M.R. Abdul Manaf, 2022. Extraction of silica from rice husk ash and its effect on the

- properties of the integral membrane. *ASM Science Journal*, vol. 17, pp. 1 - 13.
- [15] G.J. Francisco, A. Chakma, and X. Feng, 2007. Membranes comprising of alkanolamines incorporated into poly(vinyl alcohol) matrix for CO₂/N₂ separation. *Journal of Membrane Science*, vol. 303 (1), pp. 54-63.
- [16] F. F. Ghiggi, L.D. Pollo, N.S.M. Cardozo, I.C. Tessaro, 2017. Preparation and characterization of polyethersulfone/N-phthaloyl-chitosan ultrafiltration membrane with antifouling property. *European Polymer Journal*, vol. 92, pp. 61-70.
- [17] H.K. Tsade, 2016. Atomic absorption spectroscopic determination of heavy metal concentrations in Kulufo river, Arbaminch, Gamo Gofa, Ethiopia. *Journal of Environmental Analytical Chemistry*, vol. 3 (1), pp. 1-3.
- [18] N.Z. Kassim Shaari, N.A. Rahman, N.A. Sulaiman, R.M. Tajuddin, 2017. Thin film composite membranes: Mechanical and antifouling properties, in *MATEC Web Conference (ISCEE 2016)*. Malaysia, pp. 06005.
- [19] X. Zhu, H.-E. Loo, and R. Bai, 2013. A novel membrane showing both hydrophilic and oleophobic surface properties and its non-fouling performances for potential water treatment applications. *Journal of Membrane Science*, vol. 436, pp. 47-56.
- [20] Y.-H. Han, A. Taylor, M.D. Mantle, K.M. Knowles, 2007. Sol-gel-derived organic-inorganic hybrid materials. *Journal of Non-Crystalline Solids*, vol. 353 (3), pp. 313-320.
- [21] J. G. Varghese, R. S. Karuppannan, and M. Y. Kariduraganavar, 2010. Development of hybrid membranes using chitosan and silica precursors for pervaporation separation of water + isopropanol mixtures. *Journal of Chemical & Engineering Data*, vol. 55 (6), pp. 2084-2092.

- [22] A.B.D. Nandiyanto, R. Oktiani, R. Ragadhita, 2019. How to read and interpret FTIR spectroscopy of organic material. *Indonesian Journal of Science & Technology*, vol. 4 (1), pp. 97-118.
- [23] S. Ravi and M. Selvaraj, 2014. Incessant formation of chain-like mesoporous silica with a superior binding capacity for mercury. *Dalton Transactions*, vol. 43 (14), pp. 5299-5308.
- [24] T. Oh and C. K. Choi, 2010. Comparison between SiOC thin films fabricated by using plasma enhanced chemical vapor deposition and SiO₂ thin films by using fourier transform infrared spectroscopy. *Journal of the Korean Physical Society*, vol. 56 (4), pp. 1150-1155.
- [25] K. Košutić, D. Dolar, and B. Kunst, 2006. On experimental parameters characterizing the reverse osmosis and nanofiltration membranes' active layer. *Journal of Membrane Science*, vol. 282 (1), pp. 109-114.
- [26] D.A.R.O.d. Silva, L.C.B. Zuge, A.d.P. Scheer, 2020. Preparation and characterization of a novel green silica/PVA membrane for water desalination by pervaporation. *Separation and Purification Technology*, vol. 247, pp. 116852.
- [27] H.-P. Xu, Y.-H. Yu, W.-Z. Lang, X. Yan, Y.-J. Guo, 2015. Hydrophilic modification of polyvinyl chloride hollow fiber membranes by silica with a weak in situ sol-gel method. *RSC Advances*, vol. 5 (18), pp. 13733-13742.